Applied Catalysis B: Environmental 148–149 (2014) 136–143

Contents lists available at ScienceDirect

Applied Catalysis B: Environmental

journal homepage: www.elsevier.com/locate/apcatb

Review

Intrinsic kinetics in carbon gasification: Understanding linearity, "nanoworms" and alloy catalysts

Luis Sousa Lobo*

Requimte Research Center, Chemistry Department, Universidade Nova de Lisboa, 2829-516 Caparica, Portugal

ARTICLE INFO

Article history:
Received 14 June 2013
Received in revised form
13 September 2013
Accepted 28 September 2013
Available online 30 October 2013

Keywords:
Heterogeneous catalysis
Carbon gasification
Intrinsic kinetics
Alloy catalysts

ABSTRACT

There is good evidence that understanding the kinetics of catalytic carbon gasification involves the use of Fick's Law at nano-level, to evaluate the relative rates of the three main steps: (1) carbon dissolution; (2) carbon bulk diffusion through the catalyst and (3) surface reaction. Intrinsic kinetics should be handled taking that into account. When we observe linearity in the weight vs. time dependence up to more than 50% conversion this is a strong indication that a carbon bulk diffusion mechanism is operating. The peculiar behavior of moving catalyst nanoparticles observed under in-situ microscopy is also explained by the same mechanism. Occurrence of synergetic effects with alloys may be due to facilitating one or more of the three steps.

Contents

1. Introduction

In a recent review we offered evidence that dissolution of carbon and its diffusion through the catalyst particles is a key factor (as relevant as the catalytic surface activity) to allow surface reaction of the gas with dissolved carbon atoms. In the present paper we try to clarify the interpretation of experimental data of different reactions taking place either: (1) on the surface of carbon (non-catalytic gasification); (2) on the mass of carbon (pyrolisis/volatilization); (3) via carbon bulk diffusion through catalyst particles. In this case the role of the catalyst is double, involving the two sides of minute catalyst particles, in one of which carbon is continuously dissolving (solid solution)—a contact active surface area (CASA) that keeps moving.

2. Observed behavior

The behavior of the minute catalyst particles during carbon gasification has been observed by various authors. Hennig observed in 1961 that channeling of the catalyst particles on graphite is initiated only when the catalyst particle comes in contact with a step [1]. Thomas and Walker studied in 1964 the mobility of various

* Corresponding author. Tel.: +351 212948385.
E-mail address: sousalobo266@gmail.com

0926-3373
http://dx.doi.org/10.1016/j.apcatb.2013.09.048

metal particles on graphite under O_2 and CO_2 [2a]. They observed channels opened by Co particles under O_2 at 720 °C but supported the proposal by Hudson that the catalyst particles were moving on a chemisorbed layer of gas [3]. Hudson proposed equations to describe nucleation and growth of particles under a Brownian type motion behavior. McKee described how catalyst particles exhibit mobility with channeling on graphite at the same temperature that the reaction is found to start. His work in the 1970s was based on parallel observations under hot stage optical microscopy and using a microbalance (TGA) [4].

We may question whether the studies using graphite or different types of carbons and coal can be compared. There is much evidence that this is the case [5]. It is also clear that the anisotropy of the graphitic structure of carbons plays an important role. In one case the "kinetic anisotropy" was found to be 26 (ratio of the reaction rates in the *a* and *c* crystallographic directions) [2b]. The heat transfer coefficient anisotropy is also relevant here and is of the order of 100.

The overall catalytic gasification process can then be described as depicted in Fig. 1, showing a simplified view of a cut of a porous carbon grain with nanoparticles, which may start moving under reaction conditions. The diameter of the moving particles has been found to be in the range 25–140 nm by Baker (using Pd, Ni, Pt) [6] and smaller or somewhat bigger in other cases by McKee [4].

In a figurative way we may talk of this type of catalysis as being the work of particles that behave like minute woodworms or clothes moths (small animals) that eat the wood or tissue to feed themselves. Our "carbonworms" eat carbon. When the reactant gas comes in and keeps removing the feed from "behind" (back side of the moving particles) the worms keep progressing, eating more and more carbon to keep their carbon balance and so moving at a constant rate [5b].

The spillover alternative mechanism of assuming "catalyst to act as oxygen pump toward carbon" – in the words of Fino et al. [7] – is much more widely accepted, but in our view less likely. Catalytically spillover has been proposed in several cases but could not explain gasification just by carbon removal in the catalyst/carbon contact active front—not around immobile particles.

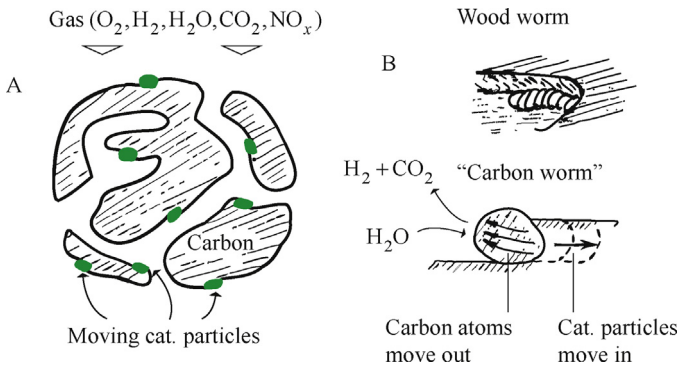

Fig. 1. *Catalyst nanoparticles.* (A) Porous carbon cut showing catalyst nanoparticles (moving under reaction conditions); (B) Analogy with a woodworm and detail of a single "carbonworm" particle. It shows the diffusion of carbon atoms through the particle in one direction and the particle itself moving in the opposite direction and keeping tight contact with carbon (into a step, corresponding to a crystallographic **a** direction).

Diffusion in chemical engineering is modeled using Fick's Law. Diffusion of carbon atoms through solids (bulk) has been known for many years in metallurgy and solid state chemistry as referred below.

3. Fast and slow moving particles

The behavior of the particles shows two alternative patterns: in some cases the smaller particles move faster, in other cases the bigger particles move faster. This was advanced as evidence that carbon bulk diffusion through the catalyst particles is operating [5,8]. When the carbon bulk diffusion step is rate limiting, the smaller particles are expected to move faster: carbon atoms have a smaller trajectory to travel. On the other hand, when the catalytic surface reaction between the reactant gas and the emerging carbon atoms is slower and rate limiting the big particles move faster, because the higher external surface is capable of handling more C atoms per unit time. The two cases are summarized in Fig. 2, showing the internal carbon concentration profile prevailing in the two cases [5a].

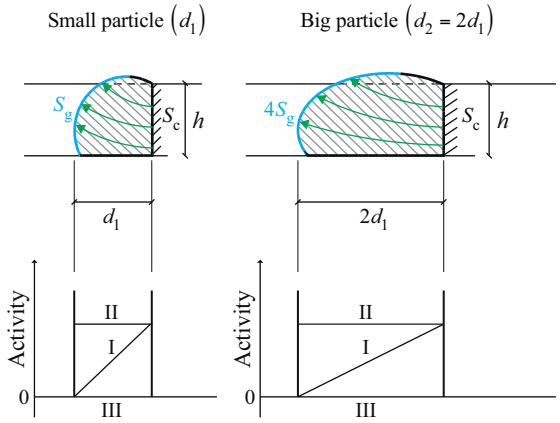

Case	Size vs speed	Carbon profile	"Slow" step	Size effect	Example	Order
A	Big = faster	II	Surface reaction	$r \sim S_g << d^2$	Ni,H_2	(1)
B	Small = faster	I	Bulk diffusion	$r \sim 1/d^x$	Ni,O_2	0
–	Independent	III	Carbon dissolution	$r \sim S_c$	–	0

Fig. 2. Expected dependence of the linear rate of gasification on particle size in accordance with the prevailing kinetics. First approach: one dimensional geometry assumed. S_g is the surface of the particle in contact with the reactant gas and h and S_c are the depth of the channel and the catalyst/carbon reaction front, respectively. For the meaning of *x* please see Lobo [5a] (modulation for two dimensions: *x* varying between 0 and 1).

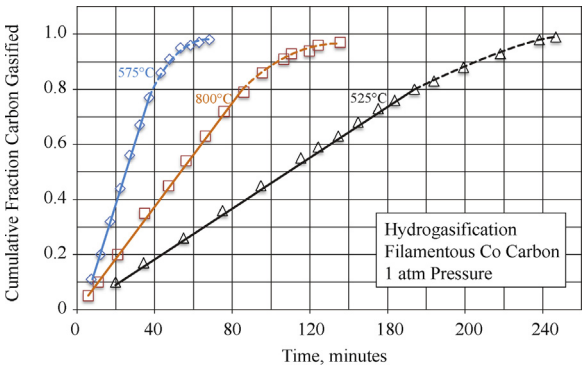

Fig. 3. *Testing linearity*: Conversion vs. time for gasification by H_2 of carbon filaments at 525°, 575° and 800 °C catalyzed by cobalt. Data from Starkovitch et al. [9]. Correlation of 1.00 to a straight line in the 0–80% portion of the data.

The table included in the figure shows the laws to be expected between particle diameter and linear rate observed by microscopy in the two cases. A one dimensional geometry was used and that use was justified. The two types of dependency have been found experimentally but no consistent explanation had been offered [6]. In the case of carbon gasification by H_2 using Ni as a catalyst the surface reaction is slow and rate controlling. The big particles move faster (Case A, Big = faster) and the travelling rate is proportionate to d^2 (surface area). With O_2 the surface reaction is fast and the bulk carbon diffusion is the controlling step (Case B, Small = faster). The travelling rate is proportional to $1/d$ for the longer diffusion distances, and similar for the short distances [5a]. On average a $1/d^x$ dependence has been found [6], with x = 0.5.

4. Observed and intrinsic kinetics

In catalytic carbon gasification the rate of reaction frequently remains constant up to 50% conversion or even more, as in the example shown in Fig. 3. The data are taken from the work of Starkovich et al. [9]. Our fitting of the data up to 80% conversion (full lines shown in the figure) gave a correlation of 1.00 to a straight line in the three cases. The first cases of observed linearity refer to work on graphite or removing carbon deposits from metal catalysts [9,11,13]. The first cases of "diagnosed" linearity in catalytic carbon/coke formation were pointed out by Figueiredo [11], Bernardo [13a] Hahn and Huttinger [12] and Silva and Lobo [14]. We presented in some detail in the late 80s the reasons in favor of a carbon bulk diffusion mechanism being operative [8,14a,c].

More recently extensive evidence was gathered in the work of Carabineiro [10]. All reactions (using CO_2, NO or NO_2) performed until full conversion showed a constant rate up to 90% conversion (3 examples out of more than 200 are shown in Fig. 4). Various other

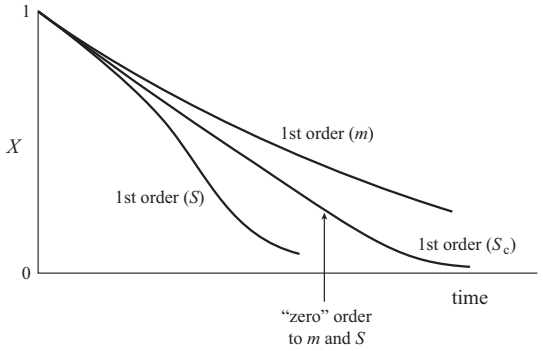

Expressing intrinsinc kinetics Proportional to:	Mass, m	Surface, S	Contact, S_c
Per unit mass of coke (pyrolosis/devolatilization)	1	–	–
Per surface area of coke (TSA, ASA, RSA)	–	1	–
Per catalyst contact active surface area (CASA)	–	–	1

Fig. 5. *Intrinsic kinetics*. Alternatives based on carbon mass (m), carbon surface (S) and catalyst contact active surface area, CASA. A straight line for the conversion/time dependence is evidence that a CASA is operating in a stable basis.

examples of publications where straight lines can be observed in the conversion vs. time record are listed in Table 1.

It makes sense to divide per m_o, the initial mass, so that the units are just t^{-1}: $r = (1/m_o)\ dm/dt$. But several authors express the rate dividing by the instant mass: $r = (1/m)\ dm/dt$. An "apparent acceleration" is then found in systems where the rate remains constant up to 90%, as shown in Fig. 4B. In several publications the linear observed change of weight with time is not shown although the presumed acceleration is represented.

The question on how to define intrinsic rate of reaction should then be raised. Fig. 5 with an adjoining table shows three alternatives. Expressing the intrinsic rate by unit surface is the obvious option for non-catalytic gasification. The alternative of using the remaining mass of carbon as a basis is justified in pyrolysis processes which are a combination of several solid state and gas–solid processes difficult to follow separately. In catalytic gasification however, the more adequate basis is the catalyst/carbon active front. The contact between catalyst and carbon along a graphene plane is usually inactive. A "lateral" contact (perpendicular to the c axis) is usually the active one, provided that carbon solubilizes easily in the catalyst at the reaction temperature.

When the reactant gas is admitted and starts removing carbon atoms by way of the catalyst surface reaction, more carbon is dissolved in the particles at the other side to approach equilibrium. This is a dynamic equilibrium sustained by a constant carbon flux. The flux should obey Fick's 2nd law during the transition (non

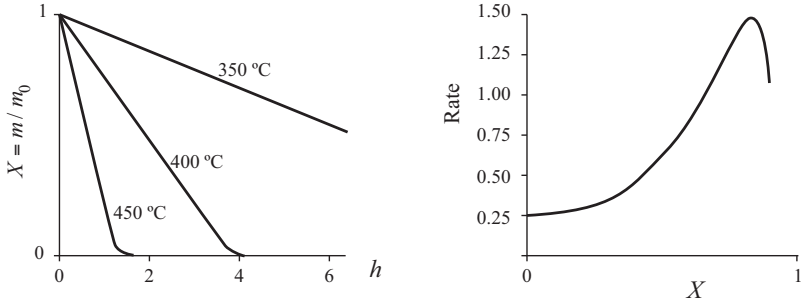

Fig. 4. *Linearity*. (A) Conversion vs. time TGA recordings for gasification of an active carbon by N_2O (0.5%N_2O in Argon) impregnated with Ba (4%) and Fe (4%) [10]; (B) Calculated "false acceleration" of the rate R (for the 400 °C run) when using intrinsic kinetics based on remaining mass: $R = dX/(1-X)dt$; $X = (m_o - m)/m_o$.

Table 1
Linearity. Examples of carbon gasification studies in which an extended period of linearity in the conversion vs. time dependence is observed. Linearity is to be expected as long as the active catalyst nanoparticles remain active and are stable: neither splitting nor merging. Carabineiro [10] used 3 gases, 9 catalysts (alone and in pairs) at various temperatures: a total of more than 1000 cases were recorded, all linear.

Carbon	Gas	Catalyst	Temp. (°C)	Linearity (%)	Year	Ref, 1st Author
Carbon deposit/Ni	H_2, H_2O	Ni	500–800	60–80	1975	[11] Figueiredo
Petroleum coke	H_2O	Fe	890–1000	50	1977	[12] Hahn
Carbon deposit/Ni	CO_2	Ni	475–775	75	1979	[13] Bernardo
Carbon filaments	H_2	Co	525–800	70	1984	[9] Starkovich
Activated carbon	CO_2	MoO_3/K_2CO_3		80	1986	[14a] Silva
Activated carbon	O_2	Mo	500	55	1990	[14c] Silva
Soot	O_2	Ca	400	50	1991	[15] Du
Sub-bituminous	NO	Ash 18.9%	700–900	60–65	1999	[16] Li
Activated carbon	CO_2	Fe, Ni, Co, Cu, Mg,	500–900	90	2000	[10] Carabineiro
Activated carbon	NO	Mn	300–900	90	2000	[10] Carabineiro
Activated carbon	N_2O	Ba,V, Pb	300–700	90	2000	[10] Carabineiro
Coals (SB, HVB)	CO_2	Ash:Fe, Na. . .	900–1100	60	2001	[17] Ochoa
Various chars	O_2	Ash	500–600	50	2002	[18] Sharma
Coal char (Illinois)	O_2	Ash	400–600	50	2008	[19] Campbell
Petroleum coke	H_2O	K_2CO_3	650–900	70–90	2011	[20] Wu

steady-state) and obey Fick's 1st law when a steady-state is operating:

$$I = -D\frac{\partial C}{\partial x} \text{ (1st law)} \quad \text{and} \quad \frac{\partial C}{\partial t} = \frac{\partial J}{\partial x} = D\frac{\partial^2 C}{\partial X^2} \text{ (2nd law)}$$

We may in short refer to that catalyst contact active surface area of all active particles as CASA, to make an analogy with the ASA an RSA concepts originally defined for non-catalytic reaction [21] but extended to catalytic reactions by Lizzio and Radovic [22].

Catalytic carbon formation and carbon gasification can be reversible processes. The gas phase side carbon activity sustained by the presence of the reactant gas dictates the direction of the carbon flux and of the movement of the particles [5,23]. Intrinsic kinetics have been expressed by different authors in various ways.

(a) Li, Radovic et al. [16] developed parallel surface area measurements to fully characterize the structure of the carbon pores and surface and of the adsorbed oxygen molecules. That approach followed previous studies and proposals by Walker et al. [21,24], Hurt, Sarofim, Du and Longwell [15,25], Lizzio and Radovic [22] (Hg porosimeter, N_2 adsorpsion, CO_2 adsorpsion, low-temperature NO chemisorption). The aim is to fully characterize the structure of the carbon pores and surface and of the adsorbed oxygen molecules. Various areas are defined: total (T), active (A), reactive (R), stable C-oxygen (O) and unoccupied (U), with the following acronyms: TSA, ASA, RSA, OASA, UASA. For true non-catalytic reactions this offers a good basis to better understand the reactivity. This treatment was extended to catalytic gasification reactions by Carberry [26] and by Lizzio and Radovic [22]. In our view this extension to catalyzed catalytic reactions is of little help and may be misleading. The same caution applies to "disguised" catalyzed reactions (catalyzed by ash impurities).

(b) Some authors reduce the modeling of the kinetics to a succession of surface reactions. This gives room for adjustment of the various parameters to fit the data, but the physical meaning of that is doubtful [27]. Moulijn and Kaptein explained the mechanism with reactivity cycles alternating free carbon sites C_f and carbon surface complexes C(O). Catalysis was explained in the following way: "The gas phase molecules are dissociated by the catalyst clusters and, as a consequence the oxygen density at the surface is increased" [28]. Therefore the role of the catalyst was judged as a spillover effect. In a more recent study the concepts of TSA and ASA were used [29].

(c) Various authors express intrinsic kinetics based on remaining carbon mass m, as referred above. The rate as a function of conversion X is then given by:

$$r = \frac{1}{1-X} \times \frac{dX}{dt}$$

with

$$X = \frac{(m_o - m)}{m_o} = \frac{1-m}{m_o}$$

This definition gives misleading results when a catalytic reaction is operating with a stable constant "front" (constant CASA). A fictitious acceleration is then "observed"–or rather inferred (see Fig. 4B). There are various examples of this false acceleration reported in the literature.

We think that the more correct way to define the intrinsic rate of catalytic carbon gasification reactions should be based in a good estimation of the catalyst contact active surface area, CASA. There are three alternatives to define the CASA front which require detailed observations and knowledge of the kinetics:

$(CASA)_{ex} = \Sigma S_{ex}$ using all the external catalyst surface (S_{ex})
$(CASA)_c = \Sigma S_c$ using the carbon/catalyst active contact (S_c)
$(CASA)_g = \Sigma S_g$ using the external active surface (S_g)

However: (1) Immobile particles (e.g. too big) are not active and must not be included; (2) When a surface catalytic solid phase is formed, different from the bulk phase in equilibrium with carbon, the separation of that area from the total external area may be difficult to estimate. It makes sense to use S_c when the bulk diffusion step is rate controlling and S_{ex} or S_g when surface reaction is rate controlling. But the difference between the alternatives is probably below the uncertainty of the calculations and so both basis are of similar value. S_{ex} is the more obvious choice, having in mind that the particles that do not have an operative S_c front should not be counted.

Some catalysts are approximately spherical particles which could offer a simple basis for a geometric estimate but others are liquid or quasi liquid spreading over carbon and the catalyst active contact area will be more difficult to estimate. Also, the size distribution of the active catalyst particles must be known. The bigger particles and particles that collide and coalesce may stay or become immobile [2]. Fino et al. concluded a gasification study with the remark: "The catalytic microstructure helps in maximizing the number of contact points between catalyst and carbon, a key step in maximizing carbon combustion" [30]. Harrisson observed in soot combustion that "maximum soot conversion is associated

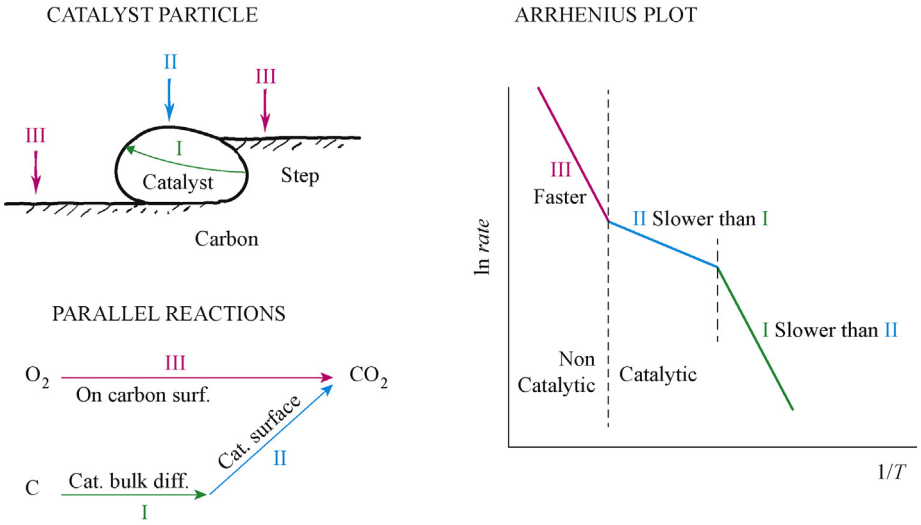

Fig. 6. Observed m (mass) vs. time dependence (half run, $t/2$) plus two sequential experiments using half the original mass ($m_0/2$). Alternatives: (I) Using half the original sample; (II) Using the half mass remaining from the 1st run. Catalyst concentration increases: 4% at the beginning, 8% at half conversion, 16% at 3/4 conversion, etc.

with better dispersion of Co_3O_4 (i.e. smaller particles)" but assumed an oxygen spillover mechanism [31].

An indication that a carbon gasification process is catalyzed by its metallic impurities is good linearity observed in the X vs. time plot. Table 1 above shows a list of cases in which that linearity was observed. In fact no explanation for the observed linearity has been advanced and it is usually ignored as a feature. We may assume that the active catalyst particles are "doing their job", at different rates according to size and kinetics, but each one at a constant rate forming together a steady global CASA front—as long as there is still enough carbon to gasify. What is changing is the "relative" load of catalyst per unit mass of carbon remaining (see Fig. 6).

A linear reaction rate may only occur when most active catalyst particles are stable in shape and composition during gasification. However, the bulk diffusion mechanism may be operating with slow catalyst changes. Therefore a non linear behavior is not proof that the carbon bulk mechanism is not operating.

A detailed analysis of the CASA front is not required to validate the concept. A researcher interested in its study should gather enough information to estimate the number, the size distribution and respective average step height distribution of the active particles. As a first step, knowing the limits of the "operative" step heights and the limits of the active particle sizes would help to model the kinetics at the nano level.

5. Temperature dependence, Arrhenius plots

The Arrhenius plots of the logarithm of the rate as a function of the reciprocal temperature is frequently used by researchers to understand the changes of the rate determining step. In series reactions the slower step prevails in the observed kinetics, while in parallel reactions the fastest one prevails and dominates the observed kinetics. A schematic summary of the two situations using parallel catalytic and non-catalytic gasification processes is shown in Fig. 7. The kinetic behavior to be expected in the various regimes is listed in Table 2, including under mass transfer limitations.

A comprehensive analysis of this type has been published recently by Senneca and Cortese [32] for coal gasification by O_2 (South African coal with 15.7% ash). A similar temperature dependency was incorrectly explained by Li et al. as a change in the rate determining step when the change should be in the reaction route (change of the dominating mechanism—in parallel reactions) [16].

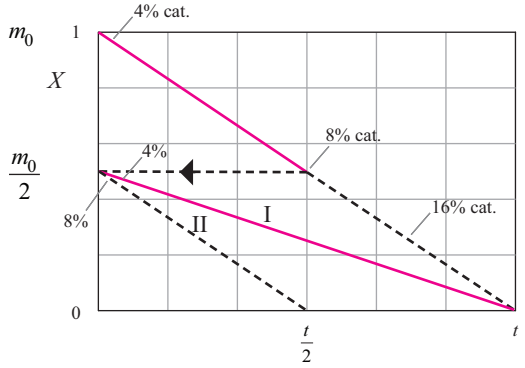

Fig. 7. *Competing reactions*. Arrhenius plot covering the competition between catalytic (steps I+II) and non-catalytic (III) gasification reaction routes. In regimens I or II the behavior of the catalyst particles is different (size effect) when observed during reaction, under in-situ microscopy (see Fig. 2).

An important point is the fact that reaction steps I and II in Fig. 7 correspond to intrinsic rates based in contact active surface area (CASA) while the parallel reaction III corresponds to reactive carbon surface area (RSA), with intrinsic rates defined differently. The linearity of the catalytic process facilitates the evaluation of reaction orders and activation energies while the rate of the non catalytic gasification route has to be referred to similar operating conditions to enable reliable estimation of orders of reaction and activation energies.

The existence of various regions in the Arrhenius plot must be analyzed considering series and parallel competition. In series competition (rate determining step) the carbon bulk diffusion step and the surface reaction step may appear in reverse order if $E_{diff} < E_a$, instead of $E_a < E_{diff}$ (please see Table). Different regimes may also correspond to independent effects of two catalysts active in different temperature windows.

Table 2
Alternative kinetic regimes and corresponding kinetic behavior.

	E_a	Order	Observations
Bulk diffusion	E_{diff}	0	Lower T
Surface reaction	E_a	n	Intermediate T
Pore diffusion	$E_a/2$	$n' = (n+1)/2$	High T
External MT	~0	1	High T, low p

In some systems maxima in the Arrhenius plots are observed [5a,9,13b,23b,59a]. The explanation advanced has usually been a thermodynamic effect in a surface reaction rate controlled process. In the case of Bernardo and Trimm using H_2 the equilibrium line of the reaction $C + 2H_2 = CH_4$ was shown to be parallel to the kinetic data plot in the high temperature regime ($T > 650\,^{\circ}C$) [13b].

6. Small catalyst particles: Nano-catalysts

The role of "ensemble size effect", shape reactivity, reconstruction and segregation phenomenon in surface nanocatalysis, all have been the object of recent attention by Uzio and Berhault [33] and Park et al. [34] and Joo et al. [35]. A 20 fold increase in rate changing the composition of bimetallic Rh/Pt catalysts or a 6 fold increase when changing the size of Ru nanoparticles (from 2 to 6 nm) have been reported. But in our case there is an extra step to care about: carbon bulk diffusion. Changes in surface structure have effect on the surface reaction but the bulk diffusivity is independent from surface changes and is in fact independent of direction for cubic structured solids (the majority, in our case). There is much research activity nowadays in this area but the dynamics of the transitions is reported by few authors.

The fact that the diffusion of carbon in metals obeys Fick's Law has been known since the early 1920s [36]. The following law applies

$$D = \frac{\nu d^2}{6} \frac{e^{-E}}{RT}$$

where d is the distance between vacancies, ν is the vibration frequency and E is the energy required for a solute atom to jump to a neighbor interstice/vacancy.

We may question whether Fick's law is still valid at nano-level and down to what level. The dependence of reaction rate on particle size when carbon bulk diffusion is thought to be controlling is apparently valid down to 25 nm [6,7]. Figueiredo and Trimm [11] used Fick's law to model the kinetics of gasification of carbon deposits on nickel catalysts. Goethel and Yang [37] used the 1st Fick's law to explain the hydrogenation of graphite catalyzed by Nickel (100–200 nm particles) and concluded that the following three modes of catalytic action observed by various authors should follow the same mechanism: monolayer channeling, deep layer channeling and bulk reaction.

Pereira et al. compared the reactivity of various carbon materials in steam gasification catalyzed by binary alloys (Ca/K and Ni/K) and found that the gas product composition was the same, which led the authors to conclude: "The same reaction mechanism appears to prevail for the catalytic gasification of graphite, chars and coals"[38].

Effective nano-catalyst particles for carbon gasification should have all the following properties:

(a) Carbon solubility,
(b) Good carbon diffusivity,
(c) Catalytic surface activity for gas/dissolved carbon reaction,
(d) Small size and stability (maximizing surface and facilitating C diffusion).

Understanding the activity of the catalyst requires solid-state knowledge. Stable small particles are of advantage, as the carbon diffusion step will be much easier and the contact surface for the surface gas reaction will be much larger. In fact, if we consider a particle splitting in 8 particles with half diameter, the total surface area doubles and the distance to be travelled by carbon atoms is halved—the total mass of catalyst is just the same. If the reaction rate is under bulk diffusion control, the diameter matters. When the surface reaction is rate controlling, the surface matters. In any case

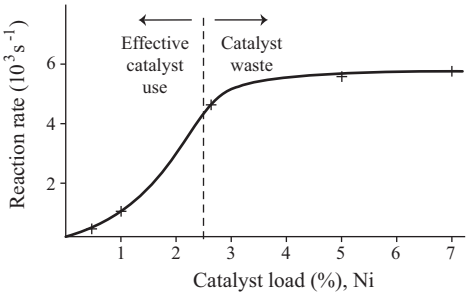

Fig. 8. Effect of catalyst load on gasification rate (Ni on active carbon, air). A saturation effect is observed above 2.5% load [14]. With higher loads we waste catalyst.

the rate doubles. An example: In reaction rates for cokes with the same amount of catalyst (%) divided either in particles having an average diameter of 100 μm or much smaller particles with 100 nm the expected difference in rate is one thousand times faster.

With a nano-catalyst the number of particles is very high. For a catalyst impregnated at a level of 4% by weight totally split in nanoparticles with an average diameter of 100 nm, the average volume of each particle will be 0.5×10^6 nm^3. In 1 cm^3 of carbon there would be about 20×10^{12} (20 trillion) particles (varying slightly with carbon porosity and metal density) assuming a complete split of the metal/alloy. However, at higher loads a wider fine split of the particles is probably more difficult to sustain and explains the maximum effective catalytic effect level observed at about 3% (see Fig. 8).

Impregnation and pyrolysis conditions influence catalyst the degrees of dispersion and interaction. Radovic et al. [39] developed a model to explain the effect of pyrolysis on subsequent CO_2 gasification catalyzed by CaO after evidence that pyrolysis residence time had a profound effect on CaO dispersion and established a correlation between a physical property (catalyst dispersion) and the observed gasification behavior of lignite chars prepared under different pyrolysis conditions. Levendis et al. [40] studied the effect method of addition and porosity: ion-exchange and large pores ensured maximum catalytic effect. The change of the catalyst from dominant $CaCO_3$ to CaO only occurred after total carbon consumption.

The hypothesis of carbon solubility having a role in the catalytic process was raised by Hahn and Huttinger in their communication to the Biennial Carbon Conference in 1977. We can check in the C–Fe phase diagram that the maximum solubility of carbon in α-iron at 738 °C is 0.02 wt% to be compared with a much higher solubility in γ-iron, increasing with temperature to reach 2% at 1150 °C (more than 100 times higher).

In their study of carbon gasification of graphite by C_2H_6/H_2O Lund et al. [41] also suggested that changes in carbon solubility could explain some of the features of the behavior observed. They observed that particles became mobile at 665 °C showing a dual morphology: "one portion of the particle was quite dense and globular" while "the remainder took the form of a thin platelet appendage". Edge recession was observed but at 870 °C the particles had a tendency to spread and wet, resulting in edge recession instead of channeling as before. At 950 °C the thin portion of the particles disappeared. Carbon bulk diffusion through both particles and liquid films were considered in our recent review on mechanisms and models for catalytic carbon gasification [5a].

As we remarked in that review, the Hedvall effect can be invoked not only to explain reactivity of solids following Arvid Hedvall proposal but also to help understanding catalysis with bulk diffusion. There is a difference though: in the reactivity of solids the effect has to do with the effectiveness of 2nd Fick's law ("penetration");

Table 3
Synergetic effects. Rates of gasification (r) observed with three different gases catalyzed by various metal pairs: $r = (1/m_o)\ dm/dt\ s^{-1} \times 10^5$. Examples of synergetic effects sometimes observed when combining two metal catalysts are shown. Metals were added at 4 wt% (4% + 4% when combined).

Rates of gasification: synergetic effect combining two catalysts (I + II)									
Gas, temperature	N_2O, 400 °C			NO, 450 °C			CO_2, 600 °C		
I/II	I	II	I + II	I	II	I + II	I	II	I + II
Ba/Pb	0.98	0.15	6*x*	0.08	0.08	15*x*	1.63	1.47	=
Fe/V	0.18	0.17	=	0.05	0.10	20*x*	1.06	0.11	6*x*
Cu/V	1.37	0.17	=	1.40	0.10	3*x*	0.05	0.11	13*x*

in catalysis with bulk diffusion a steady state is established, so Fick's 1st law applies, with constant boundary limits at the two extremes.

Some surface chemists emphasize the different activity of different crystal faces in a nano particle. It is a fact that catalytic activity changes with crystal orientation. But in the carbon bulk diffusion step crystalline orientation is indifferent. In cubic cell structures (includes the large majority of metals used in catalysis) diffusivity is the same in all six perpendicular orientations. So there are not preferred orientations in most transition metals.

7. Understanding alloy catalysts and finding more active mixtures

Mixing metals we get sometimes a higher catalytic effect than the sum of the separate effects of each metal. In the example of Fig. 4 (400 °C, N_2O, Fe/Ba) taken from the work by Carabineiro [10] the rates observed were the following (unit: $s^{-1} \times 10^5$):

Ba : 0.98 Fe + Ba : 7.25
Fe : 0.18 No catalyst : 0.01

The synergetic effect of the mixture of the two catalysts is then 7.25/(0.98 + 0.18) = 6.2.

More examples are shown in Table 3, which lists the data from experiments with three pairs of metal catalysts (separate and combined) and with 3 different gases (N_2O, NO, CO_2). The synergetic effect is present with some gases/temperatures but not with others and usually changes with temperature. Carabineiro tested 9 catalysts (Ba, Co, Cu, Fe, Mg, Mn, Ni, Pb and V), alone and in pairs (35 combinations tested). With N_2O the observed cases of synergetic effect were 9 cases at 400 °C and 31 cases (the majority of the combinations used) at 650 °C [10].

Is that effect due to: (a) Higher carbon solubility? (b) Faster bulk carbon diffusion? (c) A more active catalytic surface? (d) Good stability of smaller particles?

On the effect of alloys on surface reaction catalysis Ponec's brief review in 2001 [42] presents an excellent updated discussion on the background theory and new experimental perspectives. In our case we must consider the effect on surface reactivity but also the effect on the bulk diffusion step. Ponec draws attention to the importance of mixing enthalpy change of the alloys, with 5 sub-divisions: (1) Ideal solutions ($\Delta H = 0$); (2) Solid solutions ($\Delta H < 0$); (3) Inter-metallic compounds/ordered solutions ($\Delta H \ll 0$); (4) Mono or bi-phasic ($\Delta H < 0$); (5) Only surface alloying possible ($\Delta H \ll 0$). He also draws attention to the fact that the particle size influences the ordering of the alloy particles, the clustering of components and segregation of phases. Recently Kirshner and Kieback [43] developed a model from which they concluded that "excess carbon solubility in nanocrystalline Fe over bulk iron is proportional to the inverse grain size". When alloys are formed the existence of eutectic and eutectoid points and new phases may influence the catalytic effect. This can be tested kinetically using different proportions of the two metals and different heat treatment temperatures and times. Fino et al. [44] used the mixture $Cs_2O{\cdot}V_2O_5$ for which a eutectic is known to form at 380 °C and commented that "the formation of eutectic liquids should be a key player in this context". Similarly Badini et al. [45] studied vanadate-based catalysts for diesel soot combustion. The catalyst performance was found to be enhanced when the catalyst was dissolved in a eutectic liquid (e.g. AgCl + CsCl), which was considered likely to improve the catalyst/carbon contact conditions. In the work of Carabineiro there was no obvious evidence from in-situ XRD of new phases being formed, but a detailed microscopic study was not made [10].

Many data on alloys are available in the encyclopedic books of Hansen [46], Elliot and Shunk [47], although information on carbon solubility and diffusion is usually not given. However, there are many old and recent studies with data that show that alloying may reduce or accelerate substantially self diffusion and carbon diffusion in metals: Somoluchowski [48], Chi-Min (Fe/Ni; alternating loads)[49], Zhang (Ni/Cu)[50], Gegner (1% Cr,Mn,Mo,Ni or Si in Fe) [51], Vasilyev (Fe self-diffusion with Ni,Mo,V,Cr, Nb,Mn,Ti, Nb) [52], Kirshner (nanocrystaline α-iron) [53]. Alloying may have an effect at surface level, in which case it is the catalytic surface effect that may be the main synergetic factor. Semi-empiric analyses of surface alloy formation have been published [54,55]. Bardi reviewed about 70 pairs of metals where some degree of mixing at atomic level of the constituent elements takes place [55]. Frequently alloys are found to have superior catalytic properties as compared with pure metals [56–58].

An interesting way to estimate both carbon solubility and diffusion in metals was proposed and tested by the Lund group using TGA [59]. This may give very valuable hints when testing alloy catalyst formulations for gasification, in parallel with kinetics and microscopic observations. There is indication that the solubility of carbon in nanoparticles may be higher than in bulk metal. More elaborate alloy studies can be made using in addition to XRD, Raman spectroscopy, field emission SEM and other techniques [60].

8. Steady-state reaction conditions, thermodynamics, Gibbs's phase rule

Under steady state reaction conditions equilibrium prevails between the phases except for the phase or interface where the rate determining step is located. The Gibbs' phase rule applies: $F = C - P + 2$. So the phase in equilibrium with the gas phase is stable (or rather meta-stable) and the same is true for the phase in equilibrium with carbon. Some of the proposed mechanisms for catalytic carbon gasification are unlikely for that reason (6 out of 12 listed in a review by Moulijn and Kapteijn [61]).

Ganga Devi and Kannan used Ellingham diagrams of free energy changes (ΔG) of formation of several metal oxides and their reduction by carbon in connection with XRD studies with the aim of determining the active phases present in carboxy methyl cellulose (CMC) catalytic gasification by Cu,Ni,Co,Fe or Ca [62]. They assumed an oxygen transfer mechanism.

Assuming a carbon bulk diffusion mechanism, two different phases may coexist in the two sides of the catalyst particles. We suggest that to identify more easily the solid phases (1) in equilibrium with the gas phase and (2) in equilibrium with carbon, two in-situ XRD experiments at reaction temperature using alternative one sided "inert" conditions may be done: (1) Gas reactant and the

catalyst dispersed on an inert solid; (2) Inert gas and the catalyst normally dispersed on carbon. The inert solid may be SiO_2.

If the rate determining step is carbon bulk diffusion and two different phases prevail at the two sides, the thickness l_1 and l_2 of each phase under steady-state must obey the rule

$$\frac{D_2}{D_1} = \frac{\Delta a_1/l_1}{\Delta a_2/l2}$$

where $\Delta a_1/l_1$ and $\Delta a_2/l2$ are the slopes of the carbon activity profiles through each phase and D_1, D_2, Δa_1, Δa_2 are the diffusivities and activity gradients in each phase [5a,8]. With binary alloys the phase diagram may be complex. One phase may be liquid and the other solid. In alloys, when a new homogeneous phase is not formed and solubility is exceeded, domains of two different solid solutions may coexist, but at nano level it may be more complex. Carbon diffusivity through the more favorable phase will prevail.

9. Conclusion

There is evidence that catalytic carbon gasification usually involves carbon bulk diffusion through catalyst nanoparticles. Coupling Fick's Law with surface reaction rates using the appropriate geometry and reliable data seems to be the challenge to better understand the reaction and its kinetics. Understanding the solid state properties of alloys at nano scale will be of great help in finding more effective and less expensive catalysts.

Acknowledgments

I thank my colleague Vitor Teodoro for help in preparing this paper.

Appendix A. Supplementary data

Supplementary material related to this article can be found, in the online version, at http://dx.doi.org/10.1016/j.apcatb.2013.09.048.

References

[1] G.R. Hennig, J. Inorg. Nucl. Chem. 24 (1962) 1129–1133.
[2] (a) J.M. Thomas, P.L. Walker, J. Chem. Phys. 41 (2) (1964) 587–588;
(b) J.M. Thomas, M.M. Jones, J. Nucl. Mater. 11 (2) (1964) 236–239.
[3] J.B. Hudson, J. Phys. Chem. 67 (9) (1963) 1884–1886.
[4] (a) D.W. McKee, Carbon 8 (5) (1970) 623–626;
(b) D.W. McKee, Carbon 12 (4) (1974) 453–464;
(c) D.W. McKee, Chem. Phys. Carbon 16 (1981) 1–118.
[5] (a) L.S. Lobo, Catal. Rev. Sci. Eng. 55 (2013) 210–245;
(b) L.S. Lobo, Modelling carbon/coke gasification: CASA, contact active surface area, in: Abstr. of the 9th Int. Meeting on Catalysis and Porous Materials, Porto, May, 2013, p. 21, Edition of Soc. Portuguesa de Química.
[6] R.T.K. Baker, in: J.L. Figueiredo, J. Moulijn (Eds.), Metal Catalyzed Gasification of Graphite, in Carbon and Coal Gasification, Martinus Nijhoff Pub, 1986, pp. 231–268.
[7] D. Fino, N. Russo, C. Badini, G. Saracco, V. Specchia, AlChE J. 49 (8) (2003) 2173–2180.
[8] L.S. Lobo, Mechanism of Surface Catalysis with Bulk Diffusion in Gas/Solid Reactions (Carbon formation and Gasification, 1988, Unpublished.
[9] J.A. Starkovitch, W.-Y. Lim, H. Peng, Fuel 188 (1984) 100.
[10] S.A.C. Carabineiro, Estudos de Conversão de NO, N_2O, CO_2 e Adsorpção/Dessorpção de SO_2 Usando Catalisadores Binários suportados em Carvão Activado, in: Ph.D. Thesis, Universidade Nova de Lisboa, 2000.
[11] (a) J.L. Figueiredo, Carbon Formation in steam reforming catalysts, in: Ph.D. Thesis, Imperial College, University of London, London, 1974;
(b) J.L. Figueiredo, D.L. Trimm, J. Catal. 40 (1975) 154–159.
[12] R. Han, K.J. Huttinger, Catalysis of water vapor gasification of coke by iron, in: Proceedings of 13th Biennial Conference on Carbon, 1977, pp. 44–45.
[13] (a) C.A. Bernardo, Carbon deposition and gasification in the context of nickel catalysts, in: Ph.D., Imperial College, University of London, London, 1977;
(b) C.A. Bernardo, D.L. Trimm, Carbon 17 (1979) 115–120.
[14] (a) I.F. Silva, L.S. Lobo, Fuel 65 (1986) 1400;
(b) I.F. Silva, J.M. Encinar, S.L. Lobo, Catal. Today 7 (1990) 239–245;
(c) I.F. Silva, L.S. Lobo, J. Catal. 136 (1990) 489–495.
[15] Z. Du, A.F. Sarofim, J.P. Longwell, P.A. Mims, Energy Fuels 5 (1991) 214–221.
[16] H.Y. Li, L.R. Radovic, G.Q. Lu, V. Rudolph, Chem. Eng. Sci. 54 (1999) 4125–4136.
[17] J. Ochoa, M.C. Cassanello, P.R. Bonelli, A.L. Cukierman, Fuel Process. Technol. 74 (3) (2001) 161–176.
[18] A. Sharma, H. Kadooka, T. Kyotani, A. Tomita, Energy Fuels 16 (2002) 54–61.
[19] P.A. Campbell, R.E. Mitchell, Combust. Flame 154 (2008) 47–66.
[20] Y. Wu, J. Wang, S. Wu, S. Huang, J. Gao, Fuel Process. Technol. 92 (2011) 523–530.
[21] (a) P.L. Walker, F. Rusinko, L.G. Austin, Adv. Catal. 11 (1959) 133–221;
(b) N.R. Laine, F.J. Wastola, P.L. Walker, J. Phys. Chem. 67 (1963) 2030–2234.
[22] (a) A.A. Lizzio, L. Radovic, Ind. Eng. Chem. Res. 30 (1991) 1735–1744;
(b) A.A. Lizzio, Jiang, L.R. Radovic, Carbon (1990) 287–319.
[23] (a) J.L. Figueiredo, C.A. Bernardo, J.J.M. Orfão, Gasification of carbon deposits on metallic catalysts, in: J.L. Figueiredo, J.A. Moulijn (Eds.), NATO ASI Series. Carbon and Coal Gasification, Martinus Nijhoff Pub, Dordrecht, 1986;
(b) M.T. Tavares, C.A. Bernardo, J.L. Figueiredo, Fuel 65 (1986) 1392–1400.
[24] R.G. Jenkins, S.P. Nandi, P.L. Walker, Fuel 52 (4) (1973) 288–293.
[25] (a) R.H. Hurt, A.F. Sarofim, J.P. Longwell, Fuel 70 (1991) 1079–1082;
(b) R.H. Hurt, A.F. Sarofim, J.P. Longwell, Energy Fuels 5 (1991) 290–299.
[26] J.J. Carberry, J. Catal. 107 (1987) 248–253.
[27] P.A. Campbell, R.E. Mitchell, Combust. Flame 154 (2008) 47–66.
[28] J.A. Moulijn, F. Kapteijn, Carbon 33 (8) (1995) 1155–1165.
[29] J.P.A. Neeft, T.X. Nijhuis, E. Smakman, M. Makkee, J.A. Moulijn, Fuel 76 (12) (1997) 1129–1136.
[30] D. Fino, N. Russo, G. Saracco, V. Spechia, J. Catal. 242 (2006) 38–47.
[31] P.G. Harrisson, I.K. Ball, W. Daniell, P. Lukinkas, M. Céspedes, E.E. Miró, M.A. Ulla, Eng. J. 95 (2003) 47–55.
[32] O. Senneca, L. Cortese, Fuel 102 (2012) 751–759.
[33] D. Uzio, G. Berhault, Catal. Rev.: Sci. Eng. 52 (2010) 106–130.
[34] J.Y. Park, Y. Zhang, M. Grass, T. Zhang, G.A. Somorjai, Nano Lett. 2 (8) (2008) 673–677.
[35] S.H. Joo, J.Y. Park, G.A. Smorjai, Nano Lett. 10 (2010) 2709–2713.
[36] R.M. Barrer, Diffusion in and Through Solids, Cambridge University Press, Cambridge, 1951.
[37] (a) P.J. Gothel, R.T. Young, J. Catal. 108 (1987) 356–363;
(b) P.J. Gothel, R.T. Young, J. Catal. 119 (1) (1989) 201–214.
[38] P. Pereira, G.A. Somorjai, H. Heinemann, Energy Fuels 6 (4) (1992) 407–408.
[39] L.R. Radovic, P.L. Walker, R.G. Jenkins, Fuel 62 (2) (1983) 209–212.
[40] Y.A. Levendis, R.C. Flagan, G.R. Gavalas, Energy Fuels 3 (1) (1989) 28–37.
[41] C.R.F. Lund, R.D. Sherwood, R.T.K. Baker, J. Catal. 104 (1987) 233–236.
[42] V. Ponec, Appl. Catal., A: Gen. 222 (2001) 31–45.
[43] A. Kirchner, B. Kieback, Scr. Mater. 64 (2011) 406–409.
[44] D. Fino, N. Russo, C. Badini, G. Saracco, V. Specchia, AlChE J. 49 (8) (2003) 2173–2180.
[45] C. Badini, G. Saracco, N. Russo, C. Spechia, Catal. Lett. 69 (2000) 207–215.
[46] M. Hansen, Constitution of Binary Alloys, McGraw-Hill, New York, 1958.
[47] (a) R.P. Elliot, Constitution of Binary Alloys. 1st Supplement, McGraw-Hill, New York, 1965;
(b) F.A. Shunk, Constitution of Binary Alloys. 2nd Supplement, McGraw-Hill, New York, 1969.
[48] R. Smoluchowski, Phys. Rev. 62 (1942) 539–544.
[49] W. Tzu-Liang, W. Chi-Min, Acta Phys. Sin. 4 (1958) 354–368.
[50] J. Zhang, Oxid. Met. 70 (2008) 15–24.
[51] J. Gegner, A.A. Vasilyev, P.-J. Wilbrandt, M. Kaffenberger, MMT 2012 Conference, 2012, pp. 261–287, Paper 1.
[52] A.A. Vasilyev, S.F. Sokolov, N.G. Kolbasnikov, D.F. Sokolov, Phys. Solid State 53 (11) (2011) 2194–2200.
[53] A. Kirshner, B. Kieback, J. Nanomater. (2012).
[54] U. Bardi, Rep. Prog. Phys. 57 (1994) 939.
[55] G. Bozzolo, J. Ferrante, R. Ibañez-Meier, Surf. Sci. 35 (1996) 2–354, 577-582.
[56] J.A. Rodriguez, Surf. Sci. Rep. 24 (1996) 223–287.
[57] A. Feller, M. Claeys, E. van Setten, J. Catal. 185 (1999) 120–130.
[58] M. Corrias, Y. Kihn, P. Kalck, P. Serp, Carbon 43 (2005) 2023–2820.
[59] R.T. Young, P.J. Goethel, J.M. Schwartz, C.R.F. Lund, J. Catal. 122 (1990) 206–210.
[60] M.T. Marques, J.B. Correia, O. Conde, Scr. Mater. 50 (2004) 963–967.
[61] J.A. Moulijn, F. Kapteijn, J.L. Figueiredo, J.A. Moulijn, Catalytic gasification, in: Carbon and Coal Gasification. NATO ASI Series, Martinus Nijhoff Pub., Dordrecht, 1986.
[62] T.G. Devi, M.P. Kannan, Energy Fuels 21 (2007) 596–601.

Update

Applied Catalysis B: Environmental
Volume 162, Issue , January 2015, Page 610

DOI: https://doi.org/10.1016/j.apcatb.2014.07.015

Applied Catalysis B: Environmental 162 (2015) 610

Contents lists available at ScienceDirect

Applied Catalysis B: Environmental

journal homepage: www.elsevier.com/locate/apcatb

Erratum

Erratum to "Intrinsic kinetics in carbon gasification: Understanding linearity, "nanoworms" and alloy catalysts" [Appl. Catal. B: Environ. 148–149 (2014) 136–143]

Luis Sousa Lobo*

Requimte Research Center, Chemistry Department, Universidade Nova de Lisboa, 2829-516 Caparica, Portugal

The publisher regrets that several errors appeared in the original paper, the corrections are as follows:

(A) $J = -D\frac{\partial C}{\partial x}$ (1st law) and $\frac{\partial C}{\partial t} = \frac{\partial J}{\partial x} = D\frac{\partial^2 C}{\partial x^2}$ (2nd law)

(B) 2nd column of p. 139.

The final term of the below equation was wrong and the corrected equation is shown below:

$$r = \frac{1}{1-X} \cdot \frac{dX}{dt} \quad \text{with} \quad X = \frac{m_0 - m}{m_0} = 1 - \frac{m}{m_0}$$

(C) In the published article, artworks of Figs. 6 and 7 were not matching with their corresponding captions, i.e. artwork of Fig. 6 was rendered with the caption of Fig. 7 and artwork of Fig. 7 was rendered with the caption of Fig. 6. These artwork should be interchanged.

DOI of original article: http://dx.doi.org/10.1016/j.apcatb.2013.09.048.

* Tel.: +351 212948385.
E-mail address: sousalobo266@gmail.com

http://dx.doi.org/10.1016/j.apcatb.2014.07.015